Carbohydrate Polymers 79 (2010) 677–684

Contents lists available at ScienceDirect

Carbohydrate Polymers

journal homepage: www.elsevier.com/locate/carbpol

Structure and properties of cellulose/chitin blended hydrogel membranes fabricated via a solution pre-gelation technique

Junjie Wu [a,b], Songmiao Liang [a], Hongjun Dai [a], Xiaoyan Zhang [a], Xiaolan Yu [a], Yuanli Cai [b,*], Lina Zhang [c], Ning Wen [d,1], Bin Jiang [e,1], Jian Xu [a,*]

[a] Beijing National Laboratory for Molecular Sciences, State Key Laboratory of Polymer Physics and Chemistry, Institute of Chemistry, Chinese Academy of Sciences, Beijing 100190, China
[b] College of Chemistry, Xiangtan University, Xiangtan, Hunan 411105, China
[c] College of Chemistry and Molecular Science, Wuhan University, Wuhan 430072, China
[d] 301 Hospital, Beijing 100853, China
[e] Baoding Hospital, Baoding, Hebei 071000, China

ARTICLE INFO

Article history:
Received 25 June 2009
Received in revised form 11 September 2009
Accepted 18 September 2009
Available online 24 September 2009

Keywords:
Cellulose
Chitin
Hydrogel membrane
Pre-gelation

ABSTRACT

High-strength cellulose/chitin blended hydrogel membranes were fabricated via a solution pre-gelation method. The morphology and structure of the resultant membranes were investigated by SEM, WXRD and FTIR. The mechanical properties and permeability of the membranes were determined by tensile test and *in situ* UV–visible spectrophotometry. Instead of the loose mesh-like structure and high crystallinity of the common membranes, remarkably dense aggregation structure and low crystallinity of the novel cellulose/chitin membranes were successfully created through the solution pre-gelation process. It effectively promoted the mechanical performance of the hydrogel membranes. Moreover, the structure and properties of the membranes closely depended on the chitin content and pre-gelation temperature. Dynamic rheology studies revealed the gelation-dynamics of the mixed solution accelerated and decelerated with chitin content. ATR-FTIR results indicated nonsolvent-induced phase-separation was the main mechanism for the formation of such membranes with special structure and improved performance.

1. Introduction

Cellulose and chitin are abundant renewable resources on earth. They have some fascinating properties, e.g., biocompatible and biodegradable (Klemm, Heublein, Fink, & Bohn, 2005; Rinaudo, 2006), and thus are of considerable interests for developing environment-friendly and biocompatibility materials (El-Azzami & Grulke, 2008; Jane et al., 2007; Khan, Tare, Oreffo, & Bradley, 2009; Nogi, Iwamoto, Nakagaito, & Yano, 2009; Nogi & Yano, 2008). Unfortunately, this strong desirability to widely extend the application of cellulose and chitin remains huge challenge due to their poor solubility in many solvents (Yan, Chen, & Bangal, 2007). Recently, a milestone work in this field has been established by Zhang and coworkers, who successfully developed a series of nontoxic and recyclable cellulose aqueous solutions based on NaOH/urea and NaOH/thiourea (Zhang, Cai, & Zhou, 2005; Zhang, Ruan, & Gao, 2003). These solvent systems can effectively dissolve cellulose over a large concentration range at low temperature through forming new hydrogen bonding and inclusion complex (IC) structure (Cai et al., 2008; Lue, Zhang, & Ruan, 2007). Cellulose membranes have been prepared from the aforementioned cellulose solution via solution casting method (Ruan, Zhang, Mao, Zeng, & Li, 2004; Yang, Miyamoto, Yamane, & Okajima, 2007). Remarkable effects of coagulants, coagulant time and the concentration of cellulose on the morphology, structure and properties of the membranes have been reported (Mao, Zhou, Cai, & Zhang, 2006). The membranes obtained usually suffered from low mechanical strength at a highly hydrated state due to its loose mesh-like structure (Mao et al., 2006; Ruan et al., 2004; Yang et al., 2007). This disadvantage greatly limited the application of regenerated cellulose products in some fields especially those need high-strength cellulose at hydrated state.

As disclosed in literatures, the IC structure in cellulose solution is unstable and easy to be destroyed by changing the environment temperature or even prolonging the storage time due to the weak nature of hydrogen bonding (Cai et al., 2008; Lue et al., 2007). In such a case, the irreversible sol–gel transition of cellulose solution would occur as a result of the self-aggregation of cellulose chains (Cai & Zhang, 2006; Ruan, Lue, & Zhang, 2008; Weng, Zhang, & Ruan, 2004). Strong evidences have been shown that the obtained

* Corresponding authors. Tel./fax: +86 10 62657919.
E-mail address: jxu@iccas.ac.cn (J. Xu).
[1] Dr. Ning Wen and Associate Prof. Bin Jiang are the visiting scholars from 301 Hospital and Baoding Hospital.

0144-8617/$ - see front matter © 2009 Elsevier Ltd. All rights reserved.
doi:10.1016/j.carbpol.2009.09.022

physical gel was composed of many regular microgels (Weng et al., 2004). Enlightened by this unique gelation behavior of cellulose solution, we previously explored a solution pre-gelation technique to create novel cellulose hydrogel membranes (Liang, Zhang, Li, & Xu, 2007). In this method, cellulose hydrogel membranes were produced from weakly physical gel state rather than directly from cellulose solution by the traditional solution casting method. This pre-gelation treatment of cellulose solution resulted in a cellulose membranes with a unique microgel-aggregated structure and an improved mechanical strength at highly hydrated state.

As a continuation and extension to our previous work, we here attempt to develop novel cellulose/chitin blended hydrogel membranes via the solution pre-gelation technique. Gelation properties of the cellulose/chitin mixed solution would be distinguishing from pure cellulose solution because of the strong hydrogen-bonding interaction between cellulose and chitin (Liang, Zhang, & Xu, 2007). By using scanning electron microscopy (SEM), wide-angle X-ray diffractometry (WXRD), Fourier transform infrared spectroscopy (FTIR), tensile test and permeability test, research emphasis was focused on clarifying the effects of the chitin content and pre-gelation temperature on the structure and properties of the blended membranes. To the deep understanding on the formation mechanism of the membranes, the effect of chitin content on the gelation-dynamics of the mixed solution and the regeneration process of the physical gel in deionized water were studied by rheological test and attenuated total reflection Fourier transform infrared spectroscopy (ATR-FTIR), respectively.

2. Experimental

2.1. Materials

Cellulose (cotton linter pulp) with viscosity-average molecular weight (M_η) of 1.01×10^5 g mol^{-1} was purchased from Hubei Chem. Fiber Group, Ltd., China. Chitin with acetylation degree of 73% and M_η of 1.4×10^6 g mol^{-1} was purchased from Zhengjiang Yuhuan Co. Ltd., China. All other reagents were analytical grades, purchased from commercial sources in China.

2.2. Preparation of cellulose/chitin blended hydrogel membrane

Cotton linter (10.5 g) was dispersed in 200 g of 9.5 wt.% NaOH/4.5 wt.% thiourea aqueous solution at −8 °C and then stirred for 10 min to obtain transparent solution (**I**). 4.6 g chitin powder was immersed in 50 g of 46 wt.% NaOH aqueous solution at ambient temperature. The mixture was stored at −20 °C for 12 h. It was then warmed at room temperature and diluted by adding 175.4 g deionized water. The resultant solution was re-cooled at −20 °C for 12 h, and then was thawed and stirred vigorously at room temperature for about 30 min to obtain a 2 wt.% transparent chitin solution (**II**). Air bubbles in solution (**I**) and (**II**) were removed by centrifugation.

The preparation of the blended hydrogel membranes via solution pre-gelation method was as follow: Solution (**I**) and (**II**) were mixed at a certain weight ratio and stirred carefully to obtain a homogeneous solution. The mixed solution was then injected into square glass modules ($10 \times 10 \times 0.2$ cm^3) sealed with glass plates, and stored at a predetermined pre-gelation temperature to obtain physical gels. The pre-gelation time for those membranes was 1, 15, 7 and 7 days corresponding to the pre-gelation temperature of −20, 5, 25 and 40 °C, respectively. The obtained physical gels were taken out and dipped in deionized water to completely remove NaOH and thiourea. As a comparison, cellulose/chitin blended hydrogel membranes with different chitin content were prepared via the traditional solution casting method. Briefly, the mixed solution was cast on a glass plate with a thickness of about 1 mm, and then immediately immersed in 5 wt.% $(NH_4)_2SO_4$ aqueous solution for 10 min. Solute and coagulator in the resultant membrane were completely removed by deionized water. All membranes were stored in deionized water prior to use. The chitin content (S) in the dried membrane was calculated as follow:

$$S(\%) = \frac{W_{II} \times 2\%}{W_I \times 5\% + W_{II} \times 2\%} \times 100 \quad (1)$$

where W_I and W_{II} were the weight of original cellulose solution and chitin solution, respectively. Accordingly, the hydrogel membranes prepared from the solution pre-gelation method were coded as Px-t, where x = 0, 4.3, 9.1, 14.6 and 21 are corresponding to the chitin content of 0, 4.3, 9.1, 14.6 and 21 wt.%, respectively, and t = −20, 5, 25 and 40 are represent the pre-gelation temperature, respectively. The blended hydrogel membranes from solution casting method were denoted as Cx, where x = 0, 4.3, 9.1, 14.6 and 21 are corresponding to the chitin content of 0, 4.3, 9.1, 14.6 and 21 wt.%, respectively.

2.3. Morphology and structure characterizations

The cross-section morphology of the membrane was studied by scanning electron microscope (SEM, JSM 6700F, JEOL). The samples were frozen in liquid nitrogen, immediately snapped, and then freeze-dried under vacuum at −60 °C.

The structure of the membranes was studied by WXRD and FTIR analyses. Prior to WXRD measurements, all samples were dried at ambient temperature and ground into powder to eliminate the influence of the crystalline orientation (Yamane, Mori, Saito, & Okajima, 1996). WXRD measurement was performed on X-ray diffractometer (Riguku D/max-II, Japan) using a Cu Kα target at 40 V and 200 mA. The diffraction angle range was from 5° to 50°. FTIR spectrum of the regenerated cellulose membranes, cellulose/chitin blended membranes and pure chitin flake were recorded on a Pekin-Elmer Spectrum One FTIR Spectrometer (model 1600, Pekin-Elmer Co., USA). The test specimens were prepared by the KBr-disk method.

2.4. Mechanical test

The tensile strength (σ_b) and breaking elongation (ε_b) of the hydrogel membranes at fully hydrated state were measured on a universal tensile tester (CMT 6503, Shenzhen SANS Test machine Co. Ltd.) according to ISO527-3:1995 (E) at a speed of 5.0 mm min^{-1}. The elastic modulus (E) can be obtained from the tensile strength σ_b and the breaking elongation ε_b, as follows:

$$E = \frac{\sigma_b}{\varepsilon_b} \quad (2)$$

2.5. Drugs permeability measurement

Three model drugs, cefazidine, cefazolin sodium and thiourea, were used to determine the permeability of the blended hydrogel membranes. The physical parameters of these drugs were obtained from the literature (Liang et al., 2007). The measurements were performed using diaphragm diffusion cells made of two glass compartments (source and receiving). The hydrogel membranes were swollen in deionized water until reaching an equilibrium state, then were mounted between the two diffusion cells (the effective diffusion area was 2.11 cm^2). Subsequently, 50 mL of 2 mg/mL model drug solution was poured into the source cell and an equal volume deionized water into the receiving cell. The solutions in two cells were continuous stirring with controlled temperature (37 °C). The concentration of the drugs in receiving cell was deter-

mined *in situ* on a UV–visible spectrophotometer (Rayleigh UV-1600, China) at a predetermined interval of 5 min.

2.6. Drugs partition measurement

The partition coefficients (K_d) of cefazolin sodium between the hydrogel membranes and the soaking solutions were determined using a solution depletion method. Disk-like hydrogel membranes were immersed in drug aqueous solution (initial concentration of 2 mg/mL) at 37 °C until an equilibrium state was achieved. The membranes were then removed and the concentration of cefazolin sodium (equilibrium concentration) in the solution was determined by UV–visible spectrophotometer. All experiments were in triplicate.

2.7. Dynamic rheology

Dynamic rheology experiments were carried out on a strain controlled Advanced Rheometric Expansion System (ARES, Rheometric Scientific, NJ). Measurements were performed by using a homocentric couette with a gap of 9 mm. Strain sweeps ranging from 0% to 100% was carried out to determine the proper experimental conditions for dynamic measurements. Dynamic time sweep was then performed at the angular frequency of 1 rad/s and shear strain of 10%, which was taken well within the linear viscoelastic region. The temperature was controlled at 25 °C by a circle water bath.

2.8. ATR-FTIR spectroscopy

The measurements of hydrogel membranes were performed on a Nicolet avator 230 spectrometer at ambient temperature. The samples were taken at random from hydrogel membranes in deionized water. The residual water on the surface of samples was removed using filter papers. In direct contact with Ge crystal, data of the samples were collected over 32 scans at 4 cm^{-1} resolution using a variable-angle ATR unit (Grase by Specac Ltd.) at a nominal incident angle of 45°.

3. Results and discussion

3.1. Morphology of the blended hydrogel membranes

SEM images of the cross-section of the membranes of P*x*-*t* and C*x* are showed in Fig. 1. Under all of the considered *x*, the membrane of P*x*-5 shows denser and more homogenous morphology than that of C*x* (Fig. 1a–f). According to our previous report (Liang et al., 2007), this special structure could stem from the densely cross-linked structure of physical gel obtained during the pre-gelation process. Interestingly, regardless of the preparation method, the addition of chitin shows great ability to affect the bulk structure of the obtained hydrogel membranes. For those membranes from the solution casting method, the mesh-like structure becomes more obvious with an increased pore size and pore density at high chitin content (Fig. 1a–c). However, for those from the solution pre-gelation method, a remarkable transition of the bulk structure from dense and nonporous to mesh-like and porous is observed. P0-5 shows a nonporous aggregation structure (Fig. 1d) which is quite distinguishing from that of C0. With the addition of chitin, small pore appears in the bulk of P9.1-5, which is composed of evenly interconnected and distributed chitin/cellulose particles. These particles are cylindrical having an average diameter and average length of about 100 and 300 nm, respectively (Fig. 1e). It is striking that commonly mesh-like structure can be re-obtained by further increasing the chitin content as possessed by P21-5 (Fig. 1f). This interesting evolution in the bulk structure of P*x*-5 implies that chitin has significant effect on the sol–gel behavior of the cellulose solutions as well as their microstructure at physical gel state. This issue will be further clarified in the next section.

As that acting by the chitin content, pre-gelation temperature seems also to have meaningful effect on the bulk structure of the obtained hydrogel membranes. The membranes prepared at different pre-gelation temperature display different cross-section morphology (Fig. 1e and g–i). With the change of pre-gelation temperature, both the dense structure composed of cylindrical particles and loose mesh-like structure are obtained. P9.1-5 shows a homogenous and compact structure with some small pore in which the pore size is less than 100 nm, while P9.1-25 and P9.1-40 display relatively inhomogenous structure and their average pore size increase to about 100 and 150 nm, respectively. This result is related to the stability of IC structure during pre-gelation process (Cai et al., 2008). The IC structure is stable in solution at relatively low temperature. The slow and strong entanglements of polymer chains during pre-gelation process induce the formation of homogenous and compact structure of P9.1-5. With the increase of pre-gelation temperature, the IC structure is easier to be destroyed and the self-aggregation rate of polymer chains increases. This fast self-aggregation increases the probability of defects formation and then results in the relatively uneven structure of P9.1-25 and P9.1-40. However, we observe the mesh-like structure again in P9.1- -20. Considering the so low pre-gelation temperature of −20 °C, it is understandable. Under this condition, the solution was frozen immediately and the dispersion and conformation of polymer chains were fixed as in solution state. The slow inter- and/or intra-chain association polymer chains would not take place, causing the porous structure of P9.1- -20.

3.2. Structure of the blended hydrogel membranes

The crystal structure of cellulose and chitin in the blended membranes was studied by WAXD and the corresponding results are illustrated on Fig. 2. With four characteristic diffraction peaks at $2\theta = 9.3°$, 12.4°, 19.2° and 26.1°, pure chitin we utilized here is a typical α-chitin (Jang, Kong, Lee, & Nah, 2004). As we know, nature cellulose usually show cellulose I crystal (Otto & Spurlin, 1954). However, the membrane of P0-5 shows a typical cellulose II crystal (Kolpak & Blackwell, 1976), indicating the transformation of cellulose crystal state during the membrane preparation process.

Interestingly, the crystal behavior of cellulose and chitin in blended membranes are closely related to the preparation process, chitin content and pre-gelation temperature. The peak intensities, especially the peak at $2\theta = 11.8$ of the membranes fabricated via the solution pre-gelation method (Fig. 2c–h) are remarkably smaller than those of the membranes prepared from the solution casting method (Fig. 2b). This result suggests that the pre-gelation process efficiently suppresses the ordered packing of cellulose chains during the regeneration process and thereby forms a more homogenous blending structure with chitin. Moreover, the degree of crystallization of P9.1-5 is slightly lower than that of P0-5, indicating the addition of chitin can destroy the crystallization of cellulose. However, this decrease in the crystalline of the blended membranes in comparison with P0-5 disappears at high chitin content. As shown by the membrane of P21-5, the presence of the chitin crystal would enhance somewhat the whole crystal structure of the blended membranes. Additionally, the membrane of P9.1-5 has the lowest peak intensities and crystallinity among the membranes of P9.1-*t*. It can be explained that, at relatively low temperature, the dense physical gel is obtained due to the slow and strong entanglements of polymer chains by the pre-gelation processing. This physical gel suppresses rearrangement and limits the crystallization of polymer chains during the coagulation process.

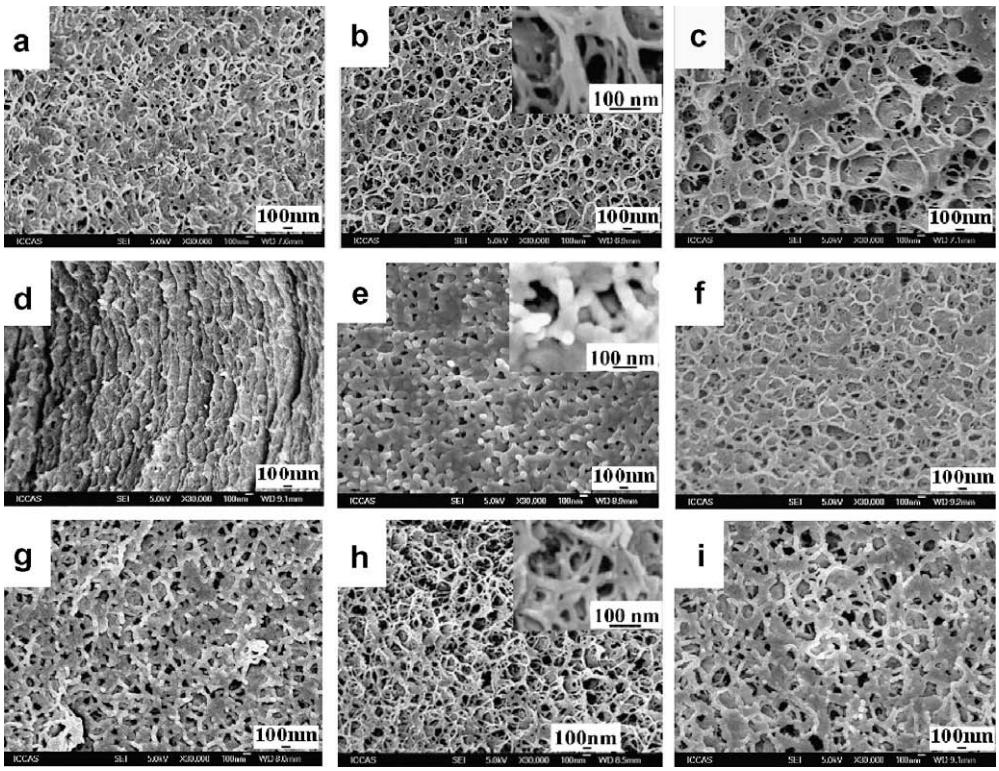

Fig. 1. SEM cross-section images of the cellulose/chitin blended membranes of C0 (a), C9.1 (b), C21 (c), P0-5 (d), P9.1-5 (e), P21-5 (f), P9.1-25 (g), P9.1- -20 (h) and P9.1-40 (i). The inserts were the amplified images.

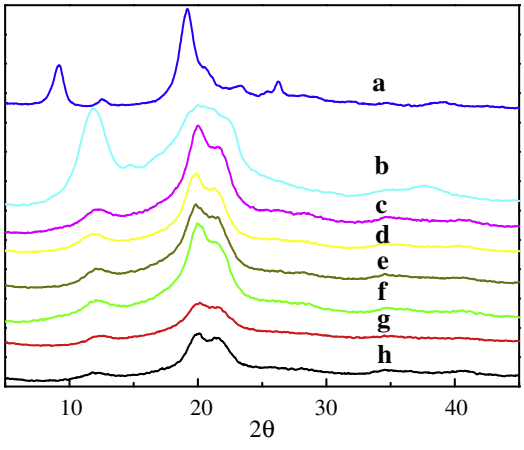

Fig. 2. WAXD patterns of the chitin flake (a) and the blended membranes of C9.1 (b), P9.1- -20 (c), P9.1-25 (d), P9.1-40 (e), P21-5 (f), P9.1-5 (g) and P0-5 (h).

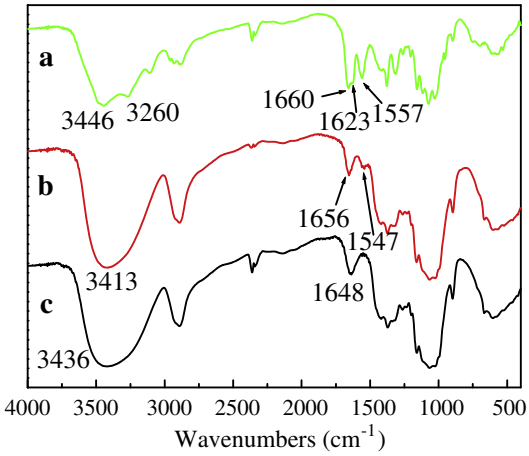

Fig. 3. FTIR spectra of the pure chitin (a), the cellulose/chitin blended membrane P9.1-5 (b), and the pure cellulose membrane P0-5 (c).

To clarify the interaction between chitin and cellulose from molecular structure, we studied the hydrogen bonding of cellulose and chitin by FTIR, as shown in Fig. 3. The absorption peak of α-chitin located at 3446 cm^{-1} is assigned to the stretching vibration of –OH. The peak centered at 3260 cm^{-1} is corresponding to the stretching vibration of –NH. Its C=O region usually composed of three sharp peaks at 1660, 1623 and 1557 cm^{-1}, which are assigned to amide I band for amorphous regions neighboring missing acetyl groups and amide II, respectively (Gow, Gooday, Russell, & Wilson, 1987). The major peak for pure cellulose membranes centered at 3436 cm^{-1} is corresponding to the stretching vibration of –OH. Compared with the chitin flake and pure cellulose membrane, the –OH stretching vibration in P9.1-5 shift to lower region (3413 cm^{-1}) and broadened. In addition, the amide II band was weakened and shifted from 1623 to 1547 cm^{-1}. These results indicate that the hydrogen bonding C=O...H–N in chitin is partially destroyed, and a new hydrogen bonding is formed between the O–H groups of cellulose and the N–H groups of chitin. This strong hydrogen-bonding interaction is related to the disparity morphology and crystal structure of blended membranes as mentioned above.

3.3. Mechanical properties of the blended hydrogel membranes

Fig. 4 presents the tensile strength and breaking elongation of the blended membranes. The tensile strength (δ_b) and the breaking elongation (ε_b) for all P*x*-5 are about 2 times larger or higher than

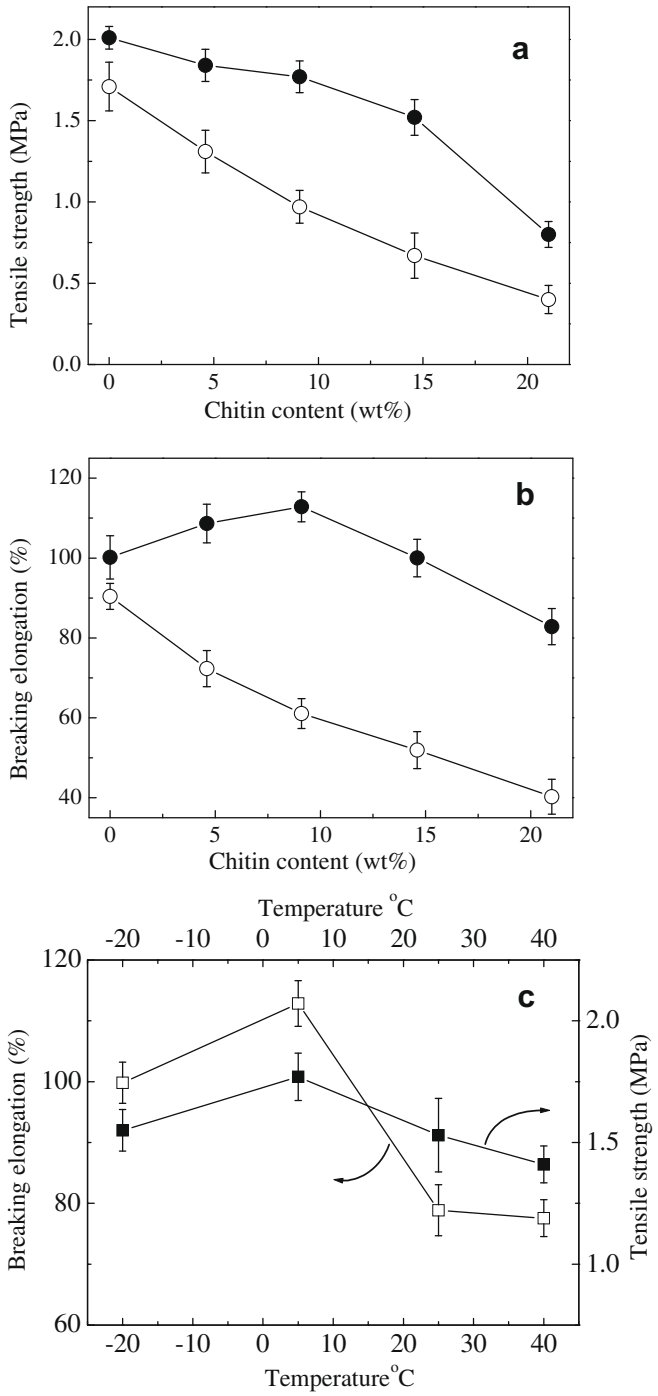

Fig. 4. Effect of chitin content on σ_b (a) and ε_b (b) of P*x*-5 (•) and C*x* (○); and effect of pre-gelation temperature on σ_b (■) and ε_b (□) of P*x*-5 (c). Error bars indicate SD.

those of C*x*, indicating an effective promotion in the mechanical performance of the hydrogel membranes is obtained by the solution pre-gelation treatment. Moreover, both δ_b and ε_b of C*x* show a monotonic and rapid decrease with the increase of the chitin content. This result arises from the formation of the loose porous structure in the C*x* with the introduction of chitin. According to Eq. (2), the elastic modulus (E) of P*x*-5 was calculated to be 2.01, 1.69, 1.57, 1.51 and 0.97 MPa, respectively. The decrease of δ_b and E of P*x*-5 with chitin content indicate that the negative effect of chitin still exist in the membranes created from solution pre-gelation method. However, the effect of chitin content on ε_b of P*x*-5 is quite interesting. As shown in Fig. 4b, instead of the above monotonic decrease, the maximum value of the breaking elongation is observed at the chitin content of 9.1 wt.%. This implies that the application of the pre-gelation treatment can effectively eliminate the negative influence of chitin on the membrane performance. The special crystal structure of the membranes of P*x*-5 could be another reason for the result. Compared the mechanical properties of the membranes with the same chitin content prepared at different pre-gelation temperature, we observe that the membrane of P9.1-5 exhibits superior mechanical property than the others (Fig. 4c). As disclosed by the morphology and structure analysis, the relatively dense bulk structure and lower crystallinity of P9.1-5 is possibly contributed to the result.

3.4. Diffusion study

In general, the drug transport process in membrane is dominated by pore mechanism and/or partition mechanism. To investigate the transport behavior of model drugs in our system, permeability and partition experiments were carried out as described. The permeability coefficient of the model drug can be calculated as follow (Gilbert, Okano, Miyata, & Kim, 1988):

$$\ln\left(\frac{1-2C_t}{C_0}\right)=\frac{2APt}{V} \tag{3}$$

Here, C_t is the drug concentration in receiving cell at time t, C_0 is the initial drug concentration in source cell, V is the solution volume in two cells and A is the effective area of permeation. The permeability coefficient (P) can be obtained from the slope of the $-(V/2A) \times ln\,(1-2C_t/C_0)$ *vs.* t plot.

The solute partition coefficient (K_d) was obtained from partition test and calculated by the following equation (He, Cao, & Lee, 2004):

$$K_d=\frac{V_s(C_i-C_s)}{V_mC_s} \tag{4}$$

Here, V_s and V_m are the volume of drug solution and swelled polymer membrane, respectively, C_i is initial drug concentration in soak solution and C_s is the equilibrium concentration in the solution.

The diffusion coefficient (D) of the drugs can be obtained from the permeability coefficient (P), solute partition coefficient (K_d) and the thickness of swelled membrane (h), following the Fick's law:

$$D=\frac{Ph}{K_d} \tag{5}$$

The permeability is defined as a particular solute through a particular membrane. Fig. 5 shows the typical $-(V/2A) \times ln\,(1-2C_t/C_0)$ *vs.* t plots of the three model drugs in the hydrogel membrane of P9.1-5. A lag region, which is regarded as the time to establish a quasi-steady state diffusion in the absence of solute–polymer interaction, exhibits in each permeability curve (Ganguly & Dash, 2004). According to the literature method (Fang, Cheng, & Lu, 1998), the lag time was estimated less than 15 min for the model drugs. By fitting the slopes of these curves, the permeability coefficients of ceftazidine, cefazolin sodium and thiourea in P9.1-5 are determined as 0.91×10^{-5}, 2.32×10^{-5} and 5.14×10^{-5} cm/s, respectively. It shows a typical degressive dependence with the increase of molecular weight or molecular radius.

Diffusion coefficient (D) is a useful parameter to estimate the ability of solutes transporting through the membrane. Based on the Eq. (5), the calculated diffusion coefficients of cefazolin sodium in P*x*-5 were listed in Table 1. The D values here ($0.75–1.26 \times 10^{-6}$ cm^2/s) are lower than our previous reported D values of cefazolin sodium within cellulose/chitin blended membranes prepared by solution casting method ($1.71–2.93 \times 10^{-6}$ cm^2/s)

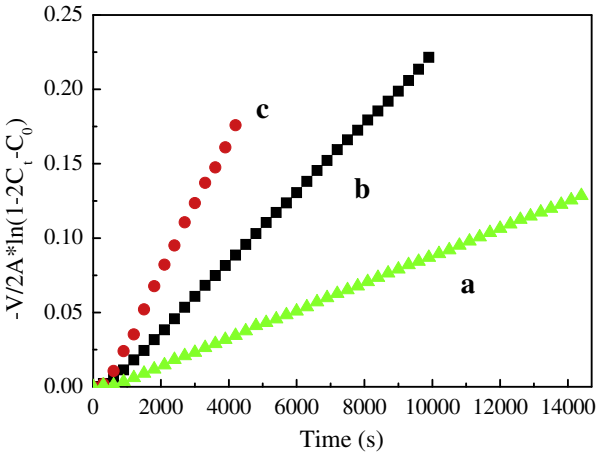

Fig. 5. Permeability of the blended hydrogel membrane of P9.1-5 to the drugs of ceftazidine (a), cefazolin sodium (b) and thiourea (c).

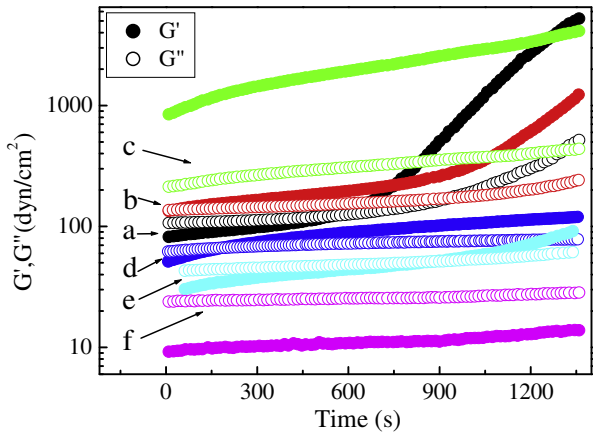

Fig. 6. Gelation kinetics in terms of the storage (G′) and loss (G″) moduli during the gelation process at the weight ratio of 2 wt.% chitin solution to 5 wt.% cellulose solution of 0:100 (a), 10:90 (b), 50:50 (c), 80:20 (d), 90:10 (e) and 100:0 (f) at 25 °C.

Table 1
Permeability (P), partition (K_d) and diffusion coefficients (D) for Cefazolin sodium across the hydrogel membranes of P*x*-5.

Sample	Permeability ($P \times 10^5$ cm/s)	Partition coefficient (K_d)	Diffusion coefficient ($D \times 10^6$ cm^2/s)
P0-5	1.84	4.93	0.75
P4.3-5	2.00	5.11	0.83
P9.1-5	2.32	5.09	0.91
P14.6-5	2.88	4.99	1.15
P21-5	3.11	5.07	1.26

(Liang et al., 2007). It is reasonable due to the bulk structure of P*x*-5 is denser than common casting membranes (Fig. 1). In addition, the permeability coefficient (P) and diffusion coefficient (D) increase with the chitin content. This result arises from the increase of pore size and porosity in the membranes by the addition of chitin (Fig. 1d–f). The transporting process of drugs dependence on pore size of membranes is well coincided with the pore mechanism.

Partition coefficient K_d is a measure of the solubility of the solute in the membrane. A low K_d value indicates a solute is not easily soluble in the membrane, while a high K_d value indicates the solute can be easily soluble in the membrane phase caused by the interactions between the solute and polymer (He et al., 2004). As shows in Table 1, although the partition coefficients show no obvious chitin content dependence, all K_d values of cefazolin sodium in the membranes P*x*-5 is high (~5). It is demonstrated that some equilibrium interactions between drug and polymer matrix, such as absorption on surface and/or active sites, are present in this system. Therefore, the partition mechanism contributes to the diffusion of the drug molecules in the membrane as well.

3.5. Formation mechanism of the blended hydrogel membranes

Our previous rheological studies demonstrated that the gelation point of cellulose aqueous solution highly depended on environmental temperature, concentration and molecular weight of cellulose. (Cai & Zhang, 2006; Ruan et al., 2008; Weng et al., 2004). Here, we focus on the effect of chitin on gelation-dynamics of mixed solution. As shown in Fig. 6, the gel time of 5 wt.% cellulose solution is about 600 s while the gel time of 2 wt.% chitin solution is lacking even after 1400 s. This result indicates that chitin solution is quite stable and possesses a slow gelation process under the test conditions. The gel time of the mixed solution at a weight ratio of chitin solution to cellulose solution of 10:90 is less than 40 s suggesting the addition of chitin into cellulose facilitate to the gelation process. Remarkably, the mixed solution at a weight ratio of chitin solution to cellulose solution of 50:50 exhibits typically elastic gel behavior during whole test process. Actually, when the weight ratio of chitin solution to cellulose solution is between 20:80 and 70:30, the gel point of these mixed solutions could not been detected during tests. This implies that a sol–gel transition of these mixed cellulose/chitin solutions occurred prior to test. The promotion of chitin on the gelation process of the mixed solution could be attributed to the strong intermolecular hydrogen bonding between cellulose and chitin.

Interestingly, the effect of chitin on the gelation process is broad-spectrum and mutual. We observed that the gel time of the mixed solution at a weight ratio of 80:20 is about 180 s. At the weight ratio of 90:10, the gel time even prolonged to 800 s. At high chitin content, although strong hydrogen-bonding interaction still presents between cellulose and chitin, the dilution of the relatively stable chitin solution on cellulose gives rise to this delay of the gel point. Because of the presence of large amount of free chitin at high content, chitin-rich region could be one of the main reasons to form the mesh-like structure of P21-5 (Fig. 1f). However, at relatively low chitin content, most of chitin chains are well interacted with cellulose and evenly dispersed in the mixture solution, promoted gelation process would cause the formation of the dense bulk structure (Fig. 1e).

Moreover, we observed that all the storage moduli (G′) except Fig. 6c at gel state decrease with the chitin percentage. In fact, the G′ of Fig. 6b increase rapidly after gelation and exceeds of Fig. 6c at the time of 1800 s (not show in Fig. 6). This is in good agreement with results of the decreasing of elastic modulus (E) obtained from tensile tests.

ATR-FTIR spectroscopy is a useful way to study the molecular structure and hydrogen bonding in hydrated samples (Hirashima, Sato, & Suzuki, 2005). Fig. 7 presents the ATR-FTIR spectra of the membrane of P9.1-5 during regeneration process. The –CO stretching of C-3 absorption peak at 1058 cm^{-1} dramatically increase with the coagulating time, demonstrating that the interaction of polymer chains is strengthened and the interaction between solvent and polymer chains is weakened (Iizuka & Aishima, 1999). This enhanced interaction is due to the destroying of the IC structure by the mutual diffusion of NaOH and thiourea in physical gel and surrounding water. The absorption peaks at 896 cm^{-1} (C–O–C stretching at the β-(1,4)-glycosidic linkage) and 2094 cm^{-1} (–CH stretching) appear and increase slightly after 30 min. These phenomena are caused by "more bonded" effect between cellulose and chitin chains at regeneration state (Ostrovskii, Kjoniksen,

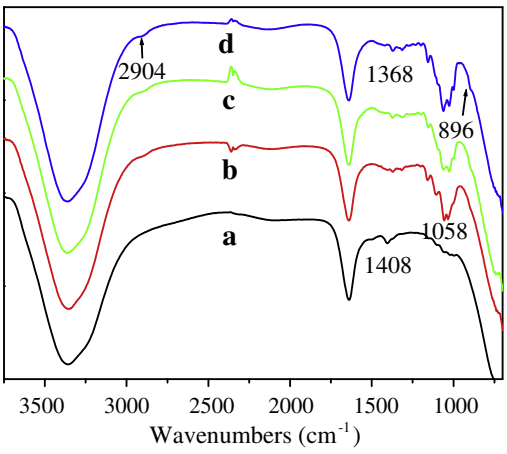

Fig. 7. ATR-FTIR spectra of the regeneration process of the cellulose/chitin blended hydrogel membrane of P9.1-5 from physical gel in deionized water with time of 0 (a), 10 (b), 30 (c) and 75 min (d).

Nystrom, & Torell, 1999). Moreover, the –CH vibration band at 1408 cm^{-1} is shift to 1367 cm^{-1}, suggesting that the transformation of cellulose crystal take place (Oh et al., 2005). These results reveal that, in the deionized water, the blended hydrogel membranes are regenerated from the gel state via nonsolvent-induced phase-separation mechanism.

On the basis of the information obtained from SEM, WXRD, FTIR, rheological results and ATR-FTIR, a schematic process describing the formation of the cellulose/chitin blended hydrogel membranes via the two methods is presented in Fig. 8. Cellulose is dissolved in aqueous solution at low temperature, due to the formation of IC structure between cellulose chains and solutes hydrates (Fig. 8a). As chitin solution is added to the cellulose solution, the IC structure in solution is partly destroyed and some physical cross-linked points are formed as a result of the strong hydrogen bonding between cellulose and chitin (Fig. 8b and d). The destroying of the IC structure in solution accelerates the sol–gel transition of mixed solution, which is confirmed by gelation-dynamics studies. At the solution state, the polymer chains in the mixed solution are still of great mobility even though strong hydrogen-bonding interaction exists between cellulose and chitin. With the solution casting method, random and rapid rearrangement of the polymer chain becomes unavoidable during the coagulation process. It therefore results in the loose mesh-like structure and high crystallization of the blended membranes as shown in C*x* (Fig. 8c). Our result indicated that this fact could be suppressed by introducing the pre-gelation treatment of the solution. In physical gel state, polymer network units are formed through slowly and strongly intermolecular association and intramolecular collapse of the polymer chains, which greatly limit the mobility and rearrangement of polymer chains (Fig. 8e). At the regeneration process, instead by a further collapse and aggregation, rearrangement of the polymer network units does not occur with the mutual diffusion of solvent and water. It is thereby favorable to obtain the blended hydrogel membranes with dense structure and low crystallization (Fig. 8f).

4. Conclusion

The solution pre-gelation method has been successfully utilized to create novel cellulose/chitin blended hydrogel membranes. All of the considered membranes showed denser structure and lower degree of crystallization compared with the membranes from traditional solution casting method. The morphology and crystal structure of those blended hydrogel membranes were tunable by chitin content and pre-gelation temperature. Distinguishing from the pore size and pore density of C*x* increasing with the chitin content, an obvious transformation from dense and nonporous to mesh-like and porous structure in P*x*-5 was observed. Similar results were obtained by changing the pre-gelation temperature. In

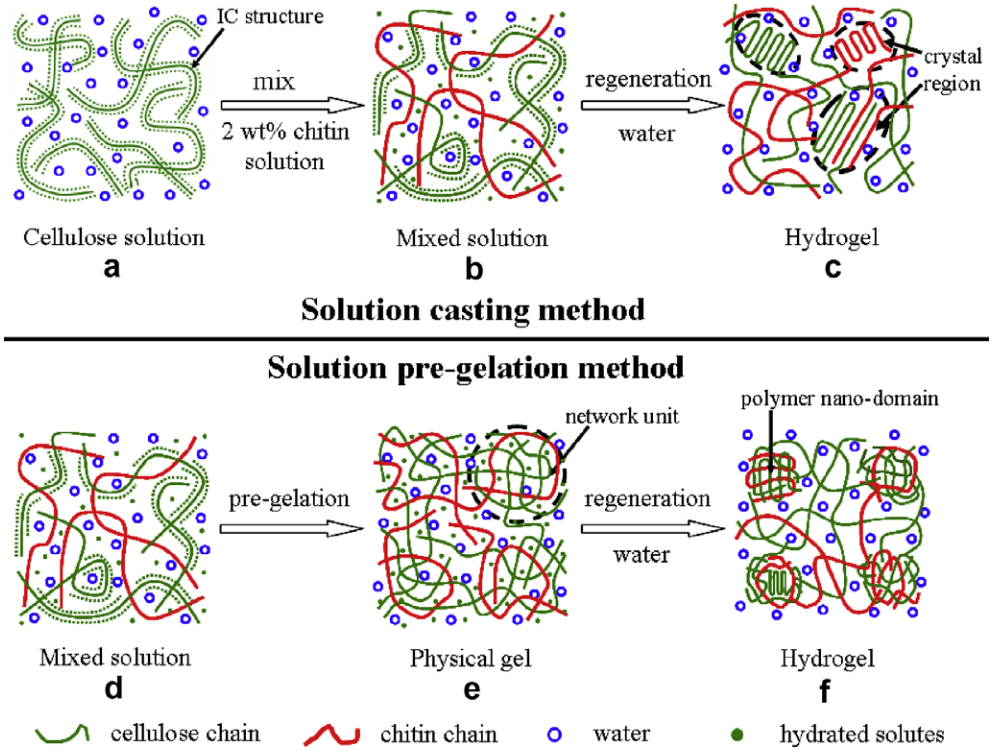

Fig. 8. Schematic fabrication processes of the cellulose/chitin blended hydrogel membranes via solution casting method (a–c) and solution pre-gelation method (d–f).

addition, the crystallinity of P*x*-5 decreased at low chitin content while increased at high chitin content. The relatively low pre-gelation temperature was also favorable for the formation of low crystallinity. The membranes of P*x*-5 displayed superior mechanical properties. Their tensile strength and breaking elongation were about 2 times larger or higher than those of C*x*. The broken elongation of P*x*-5 reached a maximum of 113% at 9.1 wt.% chitin. The diffusion of drugs through the blended hydrogel membranes prepared via solution pre-gelation method was dominated by a dual transport mechanism (pore mechanism and partition mechanism). The gelation process of the mixed solution was accelerated or decelerated depending on the chitin content in solution. The blended hydrogel membranes regenerated from the gel state in water based on the nonsolvent-induced phase-separation mechanism. These cellulose/chitin blended hydrogel membranes with special structure and improved performance have potential applications in drugs delivery devices, tissue engineering and bioseparation.

Acknowledgments

This work was supported by The National Natural Science Foundation of China (Grant Nos. 50373049, 20574076, 50425312 and 50521302), 973 Project (2007CB936400, 2005CCA00800) and Innovation Project of CAS.

References

Cai, J., & Zhang, L. N. (2006). Unique gelation behavior of cellulose in NaOH/urea aqueous solution. *Biomacromolecules, 7*, 183–189.

Cai, J., Zhang, L. N., Liu, S. L., Liu, Y. T., Xu, X. J., Chen, X. M., et al. (2008). Dynamic self-assembly induced rapid dissolution of cellulose at low temperatures. *Macromolecules, 41*, 9345–9351.

El-Azzami, L. A., & Grulke, E. A. (2008). Carbon dioxide separation from hydrogen and nitrogen by fixed facilitated transport in swollen chitosan membranes. *Journal of Membrane Science, 323*, 225–234.

Fang, Y. E., Cheng, Q. X., & Lu, B. (1998). Kinetics of in vitro drug release from chitosan/gelatin hybrid membranes. *Journal of Applied Polymer Science, 68*, 1751–1758.

Ganguly, S., & Dash, A. K. (2004). A novel in situ gel for sustained drug delivery and targeting. *International Journal of Pharmaceutics, 276*, 83–92.

Gilbert, D. L., Okano, T., Miyata, T., & Kim, S. W. (1988). Macromolecular diffusion through collagen membranes. *International Journal of Pharmaceutics, 47*, 79–88.

Gow, R. N. A., Gooday, G. W., Russell, D. G., & Wilson, M. J. (1987). Infrared and X-ray diffraction data on chitins of variable structure. *Carbohydrate Research, 165*, 105–110.

He, H., Cao, X., & Lee, L. J. (2004). Design of a novel hydrogel-based intelligent system for controlled drug release. *Journal of Controlled Release, 95*, 391–402.

Hirashima, Y., Sato, H., & Suzuki, A. (2005). ATR-FTIR spectroscopic study on hydrogen bonding of poly(*N*-isopropylacrylamide-co-soduim acrylate) gel. *Macromolecules, 38*, 9280–9286.

Iizuka, K., & Aishima, T. (1999). Starch gelation process observed by FT-IR/ATR spectrometry with multivariate data analysis. *Journal of Food Science, 64*, 653–658.

Jane, H. P., Richard, P. S., John, D. H., Scott, K. S., Andreas, M., Robin, D. R., et al. (2007). Sensor technologies based on a cellulose supported platform. *Chemical Communication, 20*, 2025–2027.

Jang, M., Kong, B. J., Lee, Y. C. H., & Nah, J. W. (2004). Physicochemical characterization of α-chitin, β-chitin, and γ-chitin separated from natural resources. *Jouranl of Polymer Science Part A: Polymer Chemistry, 42*, 3423–3432.

Khan, F., Tare, R. S., Oreffo, R. O. C., & Bradley, M. (2009). Versatile biocompatible polymer hydrogels: Scaffolds for cell growth. *Angewandte Chemie International Edition, 48*, 978–983.

Klemm, D., Heublein, B., Fink, H.-P., & Bohn, A. (2005). Cellulose: Fascinating biopolymer and sustainable raw material. *Angewandte Chemie International Edition, 44*, 3358–3393.

Kolpak, F. J., & Blackwell, J. (1976). Determination of the structure of cellulose II. *Macromolecules, 9*, 273–278.

Liang, S. M., Zhang, L. N., Li, Y. F., & Xu, J. (2007). Fabrication and properties of cellulose hydrated membrane with unique structure. *Macromolecular Chemistry and Physics, 208*, 594–602.

Liang, S. M., Zhang, L. N., & Xu, J. (2007). Morphology and permeability of cellulose/chitin blend membranes. *Journal of Membrane Science, 287*, 19–28.

Lue, A., Zhang, L. N., & Ruan, D. (2007). Inclusion complex formation of cellulose in NaOH–thiourea aqueous system at low temperature. *Macromolecular Chemistry and Physics, 208*, 2359–2366.

Mao, Y., Zhou, J. P., Cai, J., & Zhang, L. N. (2006). Effects of coagulants on porous structure of membranes prepared from cellulose in NaOH/urea aqueous solution. *Journal of Membrane Science, 279*, 246–255.

Nogi, M., Iwamoto, S., Nakagaito, A. N., & Yano, H. (2009). Optically transparent nanofiber paper. *Advanced Materials, 21*, 1595–1598.

Nogi, M., & Yano, H. (2008). Transparent nanocomposites based on cellulose produced by bacteria offer potential innovation in the electronics device industry. *Advanced Materials, 20*, 1849–1852.

Oh, S. Y., Yoo, D. Il., Shin, Y., Kim, H. C., Kim, H. Y., Chung, Y. S., et al. (2005). Crystalline structure analysis of cellulose treated with sodium hydroxide and carbon dioxide by means of X-ray diffraction and FTIR spectroscopy. *Carbohydrate Research, 340*, 2376–2391.

Ostrovskii, D., Kjoniksen, A. L., Nystrom, B., & Torell, L. M. (1999). Association and thermal gelation in aqueous mixtures of ethyl(hydroxyethyl)cellulose and ionic surfactant: FTIR and Raman study. *Macromolecules, 32*, 1534–1540.

Otto, E., & Spurlin, M. (1954). *Cellulose and cellulose derivatives* (Vol. II, p. 29). New York: Interscience.

Rinaudo, M. (2006). Chitin and chitosan: Properties and applications. *Progress in Polymer Science, 31*, 603–632.

Ruan, D., Lue, A., & Zhang, L. N. (2008). Gelation behaviors of cellulose solution dissolved in aqueous NaOH/thiourea at low temperature. *Polymer, 49*, 1027–1036.

Ruan, D., Zhang, L. N., Mao, Y., Zeng, M., & Li, X. (2004). Microporous membranes prepared from cellulose in NaOH/thiourea aqueous solution. *Journal of Membrane Science, 241*, 265–274.

Weng, L. H., Zhang, L. N., & Ruan, D. (2004). Thermal gelation of cellulose in a NaOH/thiourea aqueous solution. *Langmuir, 20*, 2086–2093.

Yamane, C., Mori, M., Saito, M., & Okajima, K. (1996). Structures and mechanical properties of cellulose filament spun from cellulose/aqueous NaOH solution system. *Polymer Journal, 28*, 1039–1047.

Yang, G., Miyamoto, H., Yamane, C., & Okajima, K. (2007). Structure of regenerated cellulose films from cellulose/aqueous NaOH solution as a function of coagulation conditions. *Polymer Journal, 39*, 34–40.

Yan, L., Chen, J., & Bangal, P. R. (2007). Dissolving cellulose in a NaOH/Thiourea aqueous solution: A topochemical investigation. *Macromolecular Bioscience, 7*, 1139–1148.

Zhang, L. N., Cai, J., & Zhou, J. P. (2005). Novel solvent compounds and theirs preparation and application. *China Patent*, Pat. No. ZL 03 128 386.1.

Zhang, L. N., Ruan, D., & Gao, S. (2003). Manufacture of cellulose film from cellulose in NaOH/thiourea aqueous solution. *China Patent*, Pat. No. ZL 00 128 216.3.